

# $J/\psi \rightarrow p\bar{p}\phi$ decay in the isobar resonance model

Jian-Ping Dai<sup>1,4,\*</sup>, Peng-Nian Shen<sup>1,2,5,6,†</sup>, Ju-Jun Xie<sup>2,3,‡</sup> and Bing-Song Zou<sup>1,2,4,5§</sup>

*1 Institute of High Energy Physics, CAS, Beijing 100049, China*

*2 Theoretical Physics Center for Science Facilities, CAS, Beijing 100049, China*

*3 Department of Physics, Zhengzhou University, Zhengzhou, Henan 450001, China*

*4 Graduate University of Chinese Academy of Sciences, Beijing 100049, China*

*5 Center of Theoretical Nuclear Physics, National Laboratory of Heavy*

*Ion Accelerator, Lanzhou 730000, China*

*6 College of Physics and Technology, Guangxi Normal University, Guilin 541004, China*

Based on the effective Lagrangian approach, the  $J/\psi \rightarrow p\bar{p}\phi$  decay is studied in an isobar resonance model with the assumption that the  $\phi$ -meson is produced from intermediate nucleon resonances. The contributions from the  $N_{1/2-}^*(1535)$ ,  $N_{3/2+}^*(1900)$ ,  $N_{1/2-}^*(2090)$  and  $N_{1/2+}^*(2100)$  states are considered. In terms of the coupling constants  $g_{\phi NN^*}^2$  and  $g_{\phi NN^*}^2$  extracted from the data of the partial decay widths of the  $N^*$ s to the  $N\pi$  channel, the reaction cross section of the  $\pi^-p \rightarrow n\phi$  process and the partial decay widths of the  $J/\psi \rightarrow p\bar{p}\eta$  and  $J/\psi \rightarrow p\bar{n}\pi^-$  processes, respectively, the invariant mass spectrum and the Dalitz plot for  $J/\psi \rightarrow p\bar{p}\phi$  are predicted. It is shown that there are two types of results. In the type I case, a large peak structure around 2.09GeV implies that a considerable amount of  $N\phi$  or  $qqqs\bar{s}$  component may exist in the narrow-width  $N_{1/2-}^*(2090)$  state, but for the wide-width  $N_{1/2+}^*(2100)$  state, it has little  $qqqs\bar{s}$  component. In the type II case, a small peak around 2.11GeV may only indicate the existence of a certain amount of  $p\phi$  or  $qqqs\bar{s}$  component in the narrow-width  $N_{1/2+}^*(2100)$  state, but no information for the wide-width  $N_{1/2-}^*(2090)$  state. Further BESIII data with high statistics would help us to distinguish the strange structures of these  $N^*$ s.

PACS numbers: 13.75.-n, 13.75.Cs, 14.20.Gk

---

\*Electronic address: daijianping@mail.ihep.ac.cn

†Electronic address: shenpn@mail.ihep.ac.cn

## I. INTRODUCTION

In past decades, many excited states of nucleon were observed and their properties, such as the mass, width, decay modes, decay branching fractions and etc., were more or less accurately measured. Most of these states and their properties can be well-explained by quark models, but some of them cannot be fitted into the nucleon spectrum predicted by the three-valence-quark model. To explain the discrepancy, except that the data is lack of higher accuracy and statistics due to the limited experimental technique and method, one speculated that these states may contain some constituents other than three  $u$  and  $d$  valance quarks, especially the  $s$  and  $\bar{s}$  quarks, and suggested to check this conjecture through experiments. Later, in the high energy physics and nuclear physics experiments, through the data analysis, one found that some excited states of nucleon ( $N^*$ ) couple strongly with strange particles. For instance, in either  $J/\psi \rightarrow \bar{p}K^+\Lambda$  decay, or  $pp \rightarrow p\Lambda K^+$  reaction near the kaon-production threshold[1, 2], or  $\gamma p \rightarrow K^+\Lambda$  kaon-photoproduction process[3–6],  $N^*(1535)$  has a significant strength of coupling to the  $K\Lambda$  channel. This indicates that the  $N^*(1535)$  state may contain a considerable mount of  $s\bar{s}$  component, which is consistent with a very large branching fraction of  $45 \sim 60\%$  for the  $N^*(1535) \rightarrow N\eta$  decay.

On the other hand, the  $\phi$ -meson is mainly composed of  $s\bar{s}$ . According to the Okubo-Zweig-Iizuka (OZI) rule [7], the production rate of  $\phi$ -meson in the nuclear process would be suppressed if the initial interacting particles do not contain a constituent with  $s$  and  $\bar{s}$  quarks. On the contrary, if a  $N^*$  contains strange constituents, its coupling with a channel involving a  $\phi$ -meson might be relatively strong. In fact, it is found that the  $pp \rightarrow pp\phi$  and  $\pi^- p \rightarrow n\phi$  reaction data can be well-explained as long as the coupling constant of  $\phi NN^*(1535)$  is sufficiently large, which implies that such a significant coupling is closely related to a fact that a considerable mount of  $s\bar{s}$  component is involved in the wave function of  $N^*(1535)$  [8]. Therefore, in the charm physics experiment at BESIII, say the measurements of  $J/\psi$  hadronic decays, the  $N\phi$  decay channel of  $J/\psi$  would also be a good place to check whether some  $N^*s$ , as the intermediate states in the decay process, have strange components, although the branching fractions of such decays are not large.

---

<sup>‡</sup>Electronic address: xiejujun@mail.ihep.ac.cn

<sup>§</sup>Electronic address: zoubs@ihep.ac.cn

Similar to  $N^*(1535)$ , some nucleon resonances which have not yet been well-established and cannot be fitted into the nucleon spectrum from theoretical models have remarkable branching fractions in some decay channels involving strange particles, say  $N\eta$ ,  $\Lambda K$  and etc. For instance, the branching fractions for  $N^*(2090) \rightarrow N\eta$ ,  $N^*(2100) \rightarrow N\eta$  and  $N^*(1900) \rightarrow N\eta$  are about 41%, 61% and 14%, respectively [19]. This implies that these states might have sizable strange constituents, and the effect of such ingredients should show up in the  $J/\psi \rightarrow p\bar{p}\phi$  decay.

In fact, the branching fraction of  $J/\psi \rightarrow p\bar{p}\phi$  was measured by the DM2 Collaboration in 1988 [9]. However, due to the insufficient statistics, no resonance information was extracted. Recently, the luminosity of BEPCII has reached over  $3 \times 10^{32} \text{cm}^{-2} \text{s}^{-1}$  around  $J/\psi$  peak, a huge amount of  $J/\psi$  events, say  $3 \times 10^9$ , will be collected at BESIII in one year. The new data set would offer an opportunity to study the possible strange ingredient or even pentaquark in the nucleon resonance.

Based on the mostly accepted assertion that the  $J/\psi \rightarrow p\bar{p}\phi$  decay is dominated by a process with intermediate nucleon resonances, so-called resonance model, we study the possibility of strange ingredients in the mentioned resonances through this decay in an effective Lagrangian approach. It is our hope that the information of the strange structure in nucleon resonances, especially those which are not well-established, can be deduced, and a reference for coming BESIII data analysis can be provided.

The paper is organized in the following way. In Section II, the theoretical model and formalism are briefly introduced. The results are presented and discussed in Section III. And in Section IV, a concluding remark is given.

## II. MODEL AND FORMALISM

In the resonance model, the  $J/\psi \rightarrow p\bar{p}\phi$  decay undergoes a two-step process, namely  $J/\psi$  firstly decays into an intermediate  $\bar{p}N^*$  ( $p\bar{N}^*$ ) state, and then  $N^*$  ( $\bar{N}^*$ ) successively decays to  $\phi$  and  $p$  ( $\bar{p}$ ). Corresponding Feynman diagrams are drawn in Fig.1, where  $k$ ,  $p_1$ ,  $p_2$ ,  $p_3$  and  $q(q')$  are the four-momenta of  $J/\psi$ ,  $p$ ,  $\bar{p}$ ,  $\phi$  and  $N^*(\bar{N}^*)$ , respectively. The embedded intermediate  $N^*$  state should have following characters. Its mass, in principle, should range from  $m_p + m_\phi$  to  $m_{J/\psi} - m_{\bar{p}}$ , namely from 1.96GeV to 2.15GeV due to the phase space restriction. However, some  $N^*$  states whose mass is smaller than the  $p\phi$  threshold

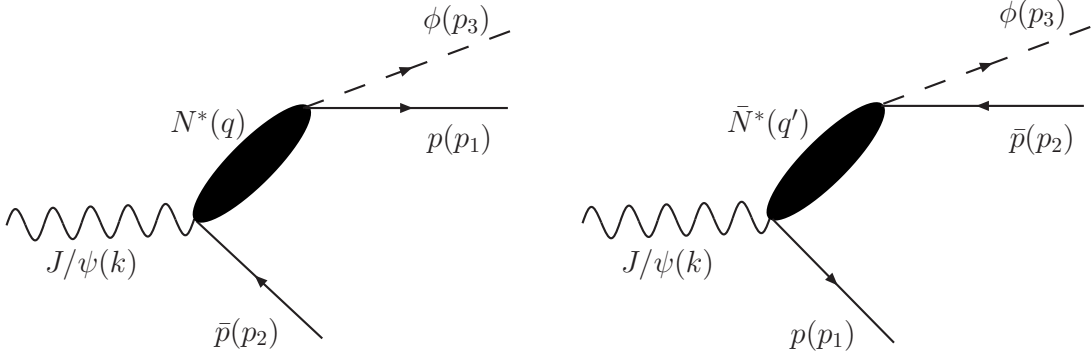


FIG. 1: Feynman diagrams for the  $J/\psi \rightarrow p\bar{p}\phi$  decay in the resonance model.

may also contribute, because of their relatively larger branching fractions for some decay channels involving strange particles and their off-shell effect as well. The spin of the intermediate  $N^*$  can be any half-integer due to a relative angular momentum between  $N^*$  and  $\bar{p}$ . For minimizing our calculation without affecting our qualitative conclusion, in the present approach, we only consider those intermediate  $N^*$  states whose contributions may dominate the decay width. Thus, the selected  $N^*$  state should have following features: It should have a relatively large branching fraction for a decay in which strange particles are involved. As a consequence, it might have, according to the OZI rule, a configuration with strangeness, so that it would be easier decaying into  $N\phi$  and relatively important in the  $J/\psi \rightarrow p\bar{p}\phi$  decay. It would also be reasonable to take the embedded  $N^*$  state with its spin up to  $5/2$  only, since the contribution from a  $N^*$  state with higher spin would encounter a power suppression due to a large relative angular momentum. In the practical calculation, in the mass region above the  $p\phi$  threshold, we only take  $N_{1/2-}^*(2090)S_{11}$  and  $N_{1/2+}^*(2100)P_{11}$  with the  $N\eta$  decay branching fractions of about 0.41 and 0.61, respectively, although the contribution from the later one would subject to a  $p$ -wave suppression, and ignore  $N_{3/2-}^*(2080)D_{13}$  and  $N_{5/2+}^*(2000)F_{15}$  because of their tiny  $N\eta$  branching fractions (about 0.03). The situation in the sub-threshold region is somewhat complex. We only take  $N_{1/2-}^*(1535)S_{11}$  and  $N_{3/2+}^*(1900)P_{13}$  into account due to their large  $N\eta$  branching fractions of about 0.45 – 0.60 and 0.14, respectively. The reason for disregarding other sub-threshold resonances like  $N_{1/2-}^*(1650)S_{11}$ ,  $N_{1/2+}^*(1710)P_{11}$ ,  $N_{3/2+}^*(1720)P_{13}$ ,  $N_{5/2+}^*(1680)F_{15}$ ,  $N_{5/2-}^*(1675)D_{15}$ ,  $N_{3/2-}^*(1520)D_{13}$ ,  $N_{1/2+}^*(1440)P_{11}$ , and  $N_{1/2+}^*(939)P_{11}$  is as follows. For  $N_{1/2-}^*(1650)S_{11}$ , its branching fractions to  $N\eta$  and  $\Lambda K$  are about 0.03~0.10 and 0.03~0.11,

respectively, which are much smaller than those for  $N_{1/2-}^*(1535)S_{11}$ . Moreover, one argued that due to the weak coupling of  $N_{1/2-}^*(1650)S_{11}$  to  $N\rho$  from SU(3) symmetry, the coupling between  $N_{1/2-}^*(1650)S_{11}$  to  $N\phi$  might also be weak [8]. In fact, if both  $N_{1/2-}^*(1535)S_{11}$  and  $N_{1/2-}^*(1650)S_{11}$  are used to fit the  $\pi^-p \rightarrow n\phi$  data, the later one would give an inappropriate contribution at the higher energies and the fitted result shows an almost zero contribution from  $N_{1/2-}^*(1650)S_{11}$  [8]. For  $N_{3/2+}^*(1720)P_{13}$ , its branching fractions to  $N\eta$  and  $\Lambda K$  are less than 0.04 and about 0.01~0.15, respectively, which are 2~3 times less than those for the  $N_{3/2+}^*(1900)P_{13}$  state. For  $N_{1/2+}^*(1710)P_{11}$ , its branching fraction to  $N\eta$  is less than 0.06, which is almost 10 times less than that for  $N_{1/2+}^*(2100)P_{11}$ , and its branching fraction to  $\Lambda K$  is about 0.05~0.25, whose largest value is about the same as that for  $N_{1/2+}^*(2100)P_{11}$ . Additionally considering the factor that  $N_{3/2+}^*(1720)P_{13}$  and  $N_{1/2+}^*(1710)P_{11}$  are the states below the  $N\phi$  threshold, their contributions would be smaller than that from  $N_{3/2+}^*(1900)P_{13}$  and much smaller than that from  $N_{1/2+}^*(2100)P_{11}$ , respectively. In fact, their contributions are evidently small near the  $N\phi$  threshold region in the  $\pi^-p \rightarrow n\phi$  reaction. For  $N_{1/2+}^*(939)P_{11}$ ,  $N_{1/2+}^*(1440)P_{11}$ ,  $N_{3/2-}^*(1520)D_{13}$ ,  $N_{5/2-}^*(1675)D_{15}$ , and  $N_{5/2+}^*(1680)F_{15}$ , their branching fractions to the  $N\eta$  channel are almost zero, and the contributions from the D-wave and F-wave states even suffer from the high-partial-wave suppression [8]. Based on such a discussion and the result given by the partial wave analysis (PWA) in Ref. [11, 12], we can safely assume that if  $N_{1/2-}^*(1535)S_{11}$ ,  $N_{3/2+}^*(1900)P_{13}$ ,  $N_{1/2-}^*(2090)S_{11}$  and  $N_{1/2+}^*(2100)P_{11}$  can give a contribution about 85% to 90% of the total, taking these four  $N^*$  states to study a system with strange particles, for instance the  $J/\psi \rightarrow p\bar{p}\phi$  process, would be meaningful. For simplicity, we omit the spectroscopic symbol in the notation of the  $N^*$  state hereafter.

To reveal the decay property of the  $J/\psi \rightarrow p\bar{p}\phi$  process, the coupling constants  $g_{\phi NN^*}$  and  $g_{\psi NN^*}$  should be fixed at the beginning.

### A. Determination of $g_{\phi NN^*}^2$

As mentioned in Ref. [8], the  $\phi$ -meson production near the threshold in the  $\pi^-p \rightarrow n\phi$  reaction is dominated by the intermediate nucleon resonances in the  $s$ -channel, and the  $u$ -channel  $N^*$  exchange and the  $t$ -channel  $\rho$ -meson exchange between pion and proton are found to be negligible, although in some references the  $t$ -channel  $\rho$ -meson exchange and/or nucleon pole contributions were assumed to be important [8, 13]. Based on this argument, the

coupling constant  $g_{\phi NN^*}^2$  can be extracted by fitting the cross section data of the  $\pi^- p \rightarrow n \phi$  reaction [8, 10]. The  $s$ -channel Feynman diagram for such a process is shown in Fig. 2, where  $p_1, p_2, p_3, p_4$ , and  $q$  denote the four-momenta of the incoming  $\pi^-$  and proton, outgoing  $\phi$  and neutron, and intermediate  $N^*$ , respectively. In this diagram, the coupling constant  $g_{\pi NN^*}^2$

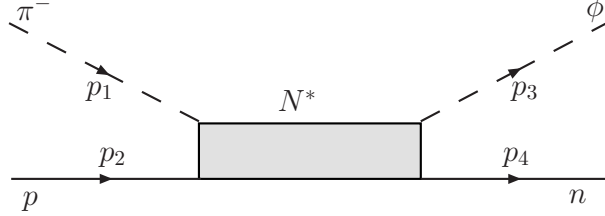


FIG. 2:  $s$ -channel Feynman diagram for the  $\pi^- p \rightarrow n \phi$  reaction in the resonance model.

( $g_{\eta NN^*}^2$ ) can be determined in terms of a commonly used effective Lagrangian [8, 14, 15]. For a nucleon resonance with  $J_{N^*}^P = \frac{1}{2}^-$  where  $J$  and  $P$  denote its spin and parity, respectively, the effective Lagrangian can be written as [8, 14, 15]

$$\mathcal{L}_{\pi NN^*} = g_{\pi NN^*} \bar{N}^* \vec{\tau} \cdot \vec{\pi} N + h.c., \quad (1)$$

with  $J_{N^*}^P = \frac{1}{2}^+$

$$\mathcal{L}_{\pi NN^*} = i g_{\pi NN^*} \bar{N}^* \gamma_5 \vec{\tau} \cdot \vec{\pi} N + h.c., \quad (2)$$

and with  $J_{N^*}^P = \frac{3}{2}^+$ , say  $N^*(1900)$ , [14]

$$\mathcal{L}_{\pi NN^*} = i \frac{g_{\pi NN^*}}{M_{N^*}} \bar{N}^{*\mu} \vec{\tau} \cdot \partial_\mu \vec{\pi} N + h.c., \quad (3)$$

where  $g_{\pi NN^*}$ ,  $N^{*\mu}$ ,  $N$ ,  $\vec{\pi}$  and  $\vec{\tau}$  denote the coupling constant of a pion to a nucleon and a  $N^*$ , the Rarita-Schwinger field of  $N^*$  with its spin of 3/2 and mass of  $M_{N^*}$ , the field of nucleon, the field of  $\vec{\pi}$  and the isospin matrices, respectively. And the effective Lagrangian for the  $\eta NN^*(1535)$  coupling can be expressed by:

$$\mathcal{L}_{\eta NN^*} = g_{\eta NN^*} \bar{N}^* \eta N + h.c.. \quad (4)$$

With these Lagrangians, the partial decay widths of the  $N^*$  states can easily be derived by evaluating the transition from the initial  $N^*$  state to the final  $N\pi$  ( $N\eta$ ) state

$$\Gamma_{N^*(1535) \rightarrow N\pi} = \frac{3g_{\pi NN^*}^2 (m_N + E_N) p_\pi^{cm}}{4\pi M_{N^*}}, \quad (5)$$

$$\Gamma_{N^*(1900) \rightarrow N\pi} = \frac{g_{\pi NN^*}^2 (m_N + E_N) (p_\pi^{cm})^3}{4\pi M_{N^*}^3}, \quad (6)$$

$$\Gamma_{N^*(2090) \rightarrow N\pi} = \frac{3g_{\pi NN^*}^2 (m_N + E_N) p_\pi^{cm}}{4\pi M_{N^*}}, \quad (7)$$

$$\Gamma_{N^*(2100) \rightarrow N\pi} = \frac{3g_{\pi NN^*}^2 (E_N - m_N) p_\pi^{cm}}{4\pi M_{N^*}}, \quad (8)$$

$$\Gamma_{N^*(1535) \rightarrow N\eta} = \frac{g_{\eta NN^*}^2 (m_N + E_N) p_\eta^{cm}}{4\pi M_{N^*}} \quad (9)$$

with

$$p_{\pi(\eta)}^{cm} = \sqrt{\frac{(M_{N^*}^2 - (m_N + m_{\pi(\eta)})^2)(M_{N^*}^2 - (m_N - m_{\pi(\eta)})^2)}{4M_{N^*}^2}}, \quad (10)$$

and

$$E_N = \sqrt{(p_{\pi(\eta)}^{cm})^2 + m_N^2}. \quad (11)$$

By re-producing the mass, the width and the  $\pi N(\eta N)$  channel branching fraction of the  $N^*$  state [19] measured in the experiment, the phenomenological coupling constant  $g_{\pi NN^*}^2$  ( $g_{\eta NN^*}^2$ ) can be extracted.

Furthermore, the effective Lagrangians of the  $\phi NN^*$  interaction for various  $N^*$  states are adopted as follows: For a  $N^*$  with  $J_{N^*}^P = \frac{1}{2}^-$ , say  $N^*(1535)$  or  $N^*(2090)$ , [8]

$$\mathcal{L}_{\phi NN^*} = g_{\phi NN^*} \bar{N}^* \gamma_5 (\gamma_\mu - \frac{q_\mu \not{q}}{q^2}) \Phi^\mu N + h.c. \quad (12)$$

with  $q$  being the four-momentum of  $N^*$  and  $\Phi^\mu$  being the field of  $\phi$  meson. For a  $N^*$  with  $J_{N^*}^P = \frac{1}{2}^+$ , say  $N^*(2100)$ ,

$$\mathcal{L}_{\phi NN^*} = g_{\phi NN^*} \bar{N}^* \gamma_\mu \Phi_\phi^\mu N + h.c., \quad (13)$$

and for a  $N^*$  with  $J_{N^*}^P = \frac{3}{2}^+$ , say  $N^*(1900)$ , [14]

$$\mathcal{L}_{\phi NN^*} = ig_{\phi NN^*} \bar{N}_\mu^* \gamma_5 \Phi_\phi^\mu N + h.c.. \quad (14)$$

To reckon for the off-shell effect of  $N^*$ , a form factor

$$F_{N^*}(q^2) = \frac{\Lambda^4}{\Lambda^4 + (q^2 - M_{N^*}^2)^2} \quad (15)$$

with  $\Lambda$  being the cut-off parameter is introduced in the  $MNN^*$  vertex [16, 17].

The propagator  $G_{JP}(q)$  of a  $N_{JP}^*$  with the quantum number  $J^P$  and momentum  $q$  can be written in a Breit-Wigner form [18]. For the  $J_{N^*} = 1/2$  state,

$$G_{\frac{1}{2}^\pm}(q) = \frac{i(\pm \not{q} + M_{N^*})}{q^2 - M_{N^*}^2 + iM_{N^*}\Gamma_{N^*}}, \quad (16)$$

where  $\Gamma_{N^*}$  denotes the total decay width of the  $N^*$  state, and the  $+$  and  $-$  signs on the left of  $\not{q}$  are the signs for the positive and negative parity states, respectively. For the  $J_{N^*} = 3/2$  state,

$$G_{\frac{3}{2}^\pm}^{\mu\nu}(q) = \frac{i(\pm \not{q} + M_{N^*})}{q^2 - M_{N^*}^2 + iM_{N^*}\Gamma_{N^*}}(-g^{\mu\nu} + \frac{1}{3}\gamma_\mu\gamma_\nu \mp \frac{1}{3M_{N^*}}(\gamma^\mu q^\nu - \gamma^\nu q^\mu) + \frac{2}{3M_{N^*}}q^\mu q^\nu). \quad (17)$$

In terms of the effective Lagrangian, form factor and  $N_{JP}^*$  propagator mentioned above, we use Feynman rules to write the invariant amplitude contributed by a  $N^*$  in the  $s$ -channel  $\pi^- p \rightarrow n\phi$  reaction as

$$\begin{aligned} \mathcal{M}_{N^*}^{\pi^- p} \propto & \sqrt{2}g_{\pi NN^*}g_{\phi NN^*}F_{N^*}(q^2)\bar{u}(p_n, s_n)\Gamma_{\phi NN^*}\varphi_\phi(p_\phi, s_\phi) \\ & G_{N^*}(q)\varphi_\pi(p_\pi, s_\pi)\Gamma_{\pi NN^*}u(p_p, s_p), \end{aligned} \quad (18)$$

where  $u$ ,  $\varphi_\phi$  and  $\varphi_\pi$  denote the fields of the nucleon,  $\phi$ -meson and  $\pi$ -meson, respectively,  $p_n$ ,  $p_p$ ,  $p_\phi$  and  $p_\pi$  represent the momenta of the proton, neutron,  $\phi$ -meson and  $\pi$ -meson, respectively,  $s_n$ ,  $s_p$ ,  $s_\phi$  and  $s_\pi$  describe the spins of the proton, neutron,  $\phi$ -meson and  $\pi$ -meson, respectively, and  $\Gamma_{\phi NN^*}$  and  $\Gamma_{\pi NN^*}$  stand for the vertex functions of  $\phi NN^*$  and  $\pi NN^*$ , respectively. The formulae of the invariant amplitude for various  $N^*$ s are given in Appendix A. Summing up all amplitudes for the  $N^*$ s considered, we obtain the total invariant amplitude

$$\mathcal{M}_{\pi^- p \rightarrow n\phi} = \sum_{N^*} \mathcal{M}_{N^*}^{\pi^- p}, \quad (19)$$

where  $N^*$  runs over all the considered states. Consequently, we can calculate the total cross section of the  $\pi^- p \rightarrow n\phi$  reaction by using the following equation

$$\sigma = \int d\Phi_2(\mathbb{P}, p_p, p_\pi, p_n, p_\phi) \frac{(2\pi)^4}{4\sqrt{(p_p \cdot p_\pi)^2 - m_p^2 m_\pi^2}} |\mathcal{M}_{\pi^- p \rightarrow n\phi}|^2, \quad (20)$$

with  $d\Phi_2$  being an element of the two-body phase space, and  $\mathbb{P}$  being the total momentum of the system. By adjusting the coupling constants  $g_{\phi NN^*}^2$  to fit the total cross section of the  $\pi^- p \rightarrow n\phi$  reaction, we can extract a set of phenomenological  $g_{\phi NN^*}^2$ . We would further mention that the contributions from the  $u$ -channel and meson-exchange channel will not be included in the calculation, because they are negligibly small [8].



## B. Determination of $g_{\psi NN^*}^2$

The coupling constant  $g_{\psi NN^*}^2$  can be extracted from the BESII data for the  $J/\psi \rightarrow p\bar{n}\pi^-$  and  $J/\psi \rightarrow p\bar{p}\eta$  decays [11, 12]. The Feynman diagrams for these decays are the same as those in Fig.1 except that the  $\phi$ -meson is replaced with the  $\pi$ - and  $\eta$ -mesons, respectively.

The effective Lagrangian for the  $J/\psi NN^*$  interaction can be chosen in the following form: For a  $N^*$  with  $J_{N^*}^P = \frac{1}{2}^-$ , say  $N^*(1535)$  or  $N^*(2090)$ , [1]

$$\mathcal{L}_{\psi NN^*} = ig_{\psi NN^*} \bar{N}^* \gamma_5 \sigma_{\mu\nu} p_\psi^\nu \epsilon^\mu(\vec{p}_\psi, s_\psi) N + h.c. \quad (21)$$

with  $p_\psi$  and  $\epsilon(p_\psi)$  being the four-momentum and the polarization vector of  $J/\psi$ , respectively, for a  $N^*$  with  $J_{N^*}^P = \frac{1}{2}^+$ , say  $N^*(2100)$ ,

$$\mathcal{L}_{\psi NN^*} = g_{\psi NN^*} \bar{N}^* \gamma_\mu \epsilon^\mu(\vec{p}_\psi, s_\psi) N + h.c., \quad (22)$$

and for a  $N^*$  with  $J_{N^*}^P = \frac{3}{2}^+$ , say  $N^*(1900)$ , [14]

$$\mathcal{L}_{\psi NN^*} = ig_{\psi NN^*} \bar{N}^* \gamma_5 \epsilon^\mu(\vec{p}_\psi, s_\psi) N + h.c.. \quad (23)$$

It should be mentioned that  $J/\psi$  meson produced in BEPCII is transversely polarized, namely  $s_3 = \pm 1$ . The completeness condition of polarization vector obeys

$$\sum_{s=\pm 1} \epsilon_\mu(\vec{p}, s) \epsilon_\nu^*(\vec{p}, s) = \delta_{\mu\nu} (\delta_{\mu 1} + \delta_{\mu 2}), \quad (24)$$

where  $\epsilon_\mu(\vec{p}, s)$ ,  $\vec{p}$  and  $s$  denote the polarization vector, the momentum, and the polarization direction of  $J/\psi$ , respectively, and  $\delta$  is a Kronecker Delta symbol.

Then, the invariant decay amplitude contributed by a specific  $N^*$  in the  $J/\psi \rightarrow p\bar{n}\pi^-$  ( $J/\psi \rightarrow p\bar{p}\eta$ ) decay can easily be written as

$$\begin{aligned} \mathcal{M}_{N^*}^{J/\psi \text{ decay}} \propto & \xi g_{\pi(\eta) NN^*} g_{\psi NN^*} F_{N^*}(q^2) \bar{u}(p_p, s_p) \Gamma_{\pi(\eta) NN^*} \varphi_{\pi(\eta)}(p_{\pi(\eta)}, s_{\pi(\eta)}) \\ & G_{N^*}(q) \varphi_\psi(p_\psi, s_\psi) \Gamma_{\psi NN^*} v(p_{\bar{p}}, s_{\bar{p}}) \end{aligned} \quad (25)$$

with  $u$  ( $v$ ) being the field of proton (anti-proton),  $\varphi_\psi$  and  $\varphi_{\pi(\eta)}$  being the fields of  $\psi$  and  $\pi(\eta)$ , respectively,  $p_p$ ,  $p_{\bar{p}}$ ,  $p_{\pi(\eta)}$  and  $p_\psi$  being the momenta of the proton, anti-proton,  $\psi$ -meson and  $\pi$ - ( $\eta$ )-meson, respectively,  $s_p$ ,  $s_{\bar{p}}$ ,  $s_{\pi(\eta)}$  and  $s_\psi$  being the spins of the proton, anti-proton,  $\psi$ -meson and  $\pi$ - ( $\eta$ )-meson, respectively, and  $\Gamma_{\pi(\eta) NN^*}$  and  $\Gamma_{\psi NN^*}$  being the vertex functions of  $\pi(\eta) NN^*$  and  $\psi NN^*$ , respectively. The coefficient  $\xi$  is taken to be  $\sqrt{2}$  for the  $p\bar{n}\pi^-$

reaction, but 1 for the  $p\bar{p}\eta$  reaction. The formulae of the invariant amplitude for various  $N^*$ s are given in Appendix B. Consequently, the total invariant amplitude can be obtained by summing over all possible  $N^*$  states

$$\mathcal{M}_{J/\psi \text{ decay}} = \frac{1}{2} \sum_{N^*} \mathcal{M}_{N^*}^{J/\psi \text{ decay}}, \quad (26)$$

where the factor of  $1/2$  comes from the average over the  $J/\psi$  spin. The partial decay width of  $J/\psi \rightarrow p\bar{n}\pi^-$  ( $J/\psi \rightarrow p\bar{p}\eta$ ) can be calculated by

$$d\Gamma = \frac{1}{2} \frac{1}{2M_\psi} \frac{p_p^0 d^3 p_p}{m_N} \frac{p_{\bar{p}}^0 d^3 p_{\bar{p}}}{m_N} \frac{d^3 p_{\pi(\eta)}}{2p_{\pi(\eta)}^0} \sum_{s_\psi} \sum_{s_p, s_{\bar{p}}, s_{\pi(\eta)}} |\mathcal{M}_{J/\psi \text{ decay}}|^2 (2\pi)^{-5} \delta^4(p_\psi - p_p - p_{\bar{p}} - p_{\pi(\eta)}). \quad (27)$$

By fitting the branching fractions of  $(2.09 \pm 0.18) \times 10^{-3}$  for  $J/\psi \rightarrow p\bar{n}\pi^-$  and  $(2.12 \pm 0.09) \times 10^{-3}$  for  $J/\psi \rightarrow p\bar{p}\eta$  [19], respectively, the magnitude of  $g_{\psi NN^*}^2$  can be extracted.

### C. $J/\psi \rightarrow p\bar{p}\phi$ decay

Using the effective Lagrangians mentioned above, the invariant amplitude of the  $J/\psi \rightarrow p\bar{p}\phi$  decay can easily be derived. Its form is the same as that in Eq.(25) except that  $\pi$  is substituted with  $\phi$

$$\begin{aligned} \mathcal{M}_{N^*}^{J/\psi \rightarrow p\bar{p}\phi} \propto & g_{\phi NN^*} g_{\psi NN^*} F_{N^*}(q^2) \bar{u}(p_p, s_p) \Gamma_{\phi NN^*} \varphi_\phi(p_\phi, s_\phi) \\ & G_{N^*}(q) \varphi_\psi(p_\psi, s_\psi) \Gamma_{\psi NN^*} v(p_{\bar{p}}, s_{\bar{p}}). \end{aligned} \quad (28)$$

The formulae of the invariant amplitude contributed by various  $N^*$ s are given in Appendix C. Then, the total invariant amplitude can be obtained by summing over the contributions from all possible  $N^*$  states

$$\mathcal{M}_{J/\psi \rightarrow p\bar{p}\phi} = \frac{1}{2} \sum_{N^*} \mathcal{M}_{N^*}^{J/\psi \rightarrow p\bar{p}\phi}, \quad (29)$$

where the factor of  $1/2$  is due to the average over the  $J/\psi$  spin as usual. The invariant mass spectrum of  $p\phi$  in the  $J/\psi \rightarrow p\bar{p}\phi$  decay can be expressed as [19]

$$\frac{d\Gamma}{d\Omega_p^* d\Omega_{\bar{p}}} = \frac{1}{2} \frac{1}{(2\pi)^5} \frac{(2m_p)^2}{16M_\psi^2} |\mathcal{M}_{J/\psi \rightarrow p\bar{p}\phi}|^2 |p_p^*| |\bar{p}| dm_{p\phi}, \quad (30)$$

where  $(|p_p^*|, \Omega_p^*)$  is the momentum of proton in the rest frame of  $p$  and  $\phi$ , and  $d\Omega_{\bar{p}}$  is the angle of anti-proton in the rest frame of the decaying  $J/\psi$ . Integrating over all the angles in the rest frame of  $J/\psi$ , the Dalitz plot can be derived in the following form [19]

$$d\Gamma = \frac{1}{2} \frac{1}{(2\pi)^3} \frac{(2m_p)^2}{32M_\psi^3} |\mathcal{M}_{J/\psi \rightarrow p\bar{p}\phi}|^2 dm_{p\phi}^2 dm_{\bar{p}\phi}^2, \quad (31)$$

with

$$m_{p\phi}^2 = p_{p\phi}^2 = (p_\psi - p_{\bar{p}})^2, \quad m_{\bar{p}\phi}^2 = p_{\bar{p}\phi}^2 = (p_\psi - p_p)^2. \quad (32)$$

### III. RESULTS AND DISCUSSION

Based on the discussion in the last section, only  $N_{1/2-}^*(1535)$ ,  $N_{3/2+}^*(1900)$ ,  $N_{1/2-}^*(2090)$  and  $N^*(2100)P_{11}$  are adopted as the intermediate state in the practical calculation. The coupling constant  $g_{\pi(\eta)NN^*}$  for these  $N^*$ s are extracted by using the decay width formulas for  $N^* \rightarrow N\pi(\eta)$  shown in the last section, where the masses of  $N$ ,  $N^*$ ,  $\pi$  and  $\eta$  are taken from PDG [19], namely  $m_N=0.938\text{GeV}$ ,  $m_\pi=0.139\text{GeV}$  and  $m_\eta=0.547\text{GeV}$ ,  $M_{N^*(1535)}=1.535\text{GeV}$ ,  $M_{N^*(1900)}=1.900\text{GeV}$ ,  $M_{N^*(2090)}=2.090\text{GeV}$ , and  $M_{N^*(2100)}=2.100\text{GeV}$ , respectively [19].

It should be noted that the total width and the branching fractions of  $N_{S_{11}}^*(1535)$  (or the partial decay widths) for the  $N\pi$  and  $N\eta$  channels have more or less accurately been measured, thus  $g_{\pi NN^*(1535)}^2$  and  $g_{\eta NN^*(1535)}^2$  can be estimated by using the averaged values of branching fractions given in PDG [19]. However, for the two-star state  $N_{3/2+}^*(1900)$  and one-star states  $N_{1/2-}^*(2090)$  and  $N_{1/2+}^*(2100)$ , their partial decay widths for the  $N\pi$  channel have not precisely been confirmed yet. The extracted  $g_{\pi NN^*}^2$  would be allowed to change in a range due to the mentioned large uncertainty. The range can roughly be estimated by using the maximal and minimal values [19] of the total width and the  $N\pi$  branching fraction for the corresponding  $N^*$ . The extracted  $g_{\pi NN^*}^2$  and  $g_{\eta NN^*}^2$  for each  $N^*$  are tabulated in Table I. From this table, it is clearly shown that the result is reasonable, namely it consists with the fact that the larger the partial decay width is, the stronger the  $N^*$  couples to the decayed particles.

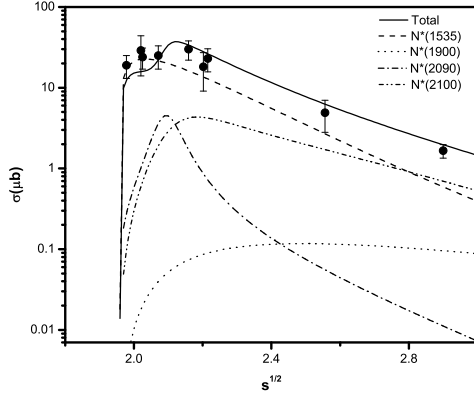
Then the coupling constants  $g_{\phi NN^*}$  for various  $N^*$ s can be extracted by fitting the total cross section data for the  $\pi^- p \rightarrow n\phi$  reaction. To consider the off-shell effect of  $N^*$ , a form factor in Eq.(15) with a cut-off parameter  $\Lambda$  being  $1.8\text{GeV}$  for  $N_{1/2-}^*(1535)$  and  $2.3\text{GeV}$  for  $N_{3/2+}^*(1900)$ ,  $N_{1/2-}^*(2090)$  and  $N_{1/2+}^*(2100)$  is employed.

TABLE I: Coupling constants  $g_{\pi NN^*}^2$  and  $g_{\eta NN^*}^2$  for various  $N^*$  states.

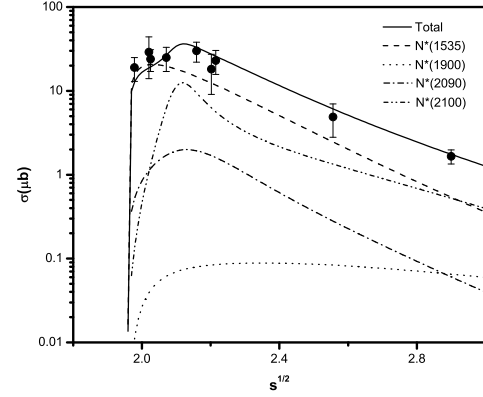
$N$	total width (GeV)[19]	decay mode	branching fraction [19]	partial width (GeV)	$g_{\pi NN^*}^2$ ( $g_{\eta NN^*}^2$ )
$N_{1/2-}^*(1535)$	0.150	$N\pi$	45%	$0.675 \times 10^{-1}$	0.468
	0.150	$N\eta$	53%	$0.795 \times 10^{-1}$	$0.431 \times 10^1$
$N_{3/2+}^*(1900)$	0.180	$N\pi$	5.5%	$0.990 \times 10^{-2}$	$0.113 \times 10^1$
	0.498	$N\pi$	26%	0.129	$0.147 \times 10^2$
$N_{1/2-}^*(2090)$	0.095	$N\pi$	9.0%	$0.855 \times 10^{-2}$	$0.410 \times 10^{-1}$
	0.350	$N\pi$	18%	$0.630 \times 10^{-1}$	0.305
	0.414	$N\pi$	10%	$0.414 \times 10^{-1}$	0.200
$N_{1/2+}^*(2100)$	0.113	$N\pi$	15%	$0.170 \times 10^{-1}$	0.564
	0.200	$N\pi$	10%	$0.200 \times 10^{-1}$	0.666
	0.260	$N\pi$	12%	$0.312 \times 10^{-1}$	$0.104 \times 10^1$

Because the magnitudes of  $g_{\pi NN^*}^2$  for the  $N_{3/2+}^*(1900)$ ,  $N_{1/2-}^*(2090)$  and  $N_{1/2+}^*(2100)$  states can respectively vary in a rather large range of their own, we combine possible  $g_{\pi NN^*}^2$  values for these  $N^*$ s into various cases to fit the reaction data. The fitted result shows that only two types of combinations can give the best fit. In type I, one can only take a smaller total width for  $N_{1/2-}^*(2090)$  and a larger total width for  $N_{1/2+}^*(2100)$ , and in type II, it is the other way round. To be specific, the restricted regions of the total widths for  $N_{3/2+}^*(1900)$ ,  $N_{1/2-}^*(2090)$  and  $N_{1/2+}^*(2100)$  are bound by the following combined cases:  $\Gamma_{N^*(1900)}/\Gamma_{N^*(2090)}/\Gamma_{N^*(2100)} = 180\text{MeV}/95\text{MeV}/200\text{MeV}$ ,  $180\text{MeV}/95\text{MeV}/260\text{MeV}$ ,  $498\text{MeV}/95\text{MeV}/200\text{MeV}$ , and  $498\text{MeV}/95\text{MeV}/260\text{MeV}$  in type I, and  $180\text{MeV}/350\text{MeV}/113\text{MeV}$ ,  $180\text{MeV}/414\text{MeV}/113\text{MeV}$ ,  $498\text{MeV}/350\text{MeV}/113\text{MeV}$  and  $498\text{MeV}/414\text{MeV}/113\text{MeV}$  in type II. The typical fitted curves of these two types are plotted in Figs. 3 (a) and (b) with  $\chi^2$  being 3.62 and 3.05, respectively. In these figures, the dashed, dotted, dash-dotted and dash-double-dotted curves denote the contributions from individual  $N_{1/2-}^*(1535)$ ,  $N_{3/2+}^*(1900)$ ,  $N_{1/2-}^*(2090)$  and  $N_{1/2+}^*(2100)$  states, respectively. The contributions from interference terms in these cases are shown in Figs. 3 (c) and (d), respectively. In these figures, we only plot the the contributions from the interference term between  $N_{1/2-}^*(1535)$  and  $N_{1/2-}^*(2090)$  and from the sum of the rest terms, shown as the solid and dashed curves,

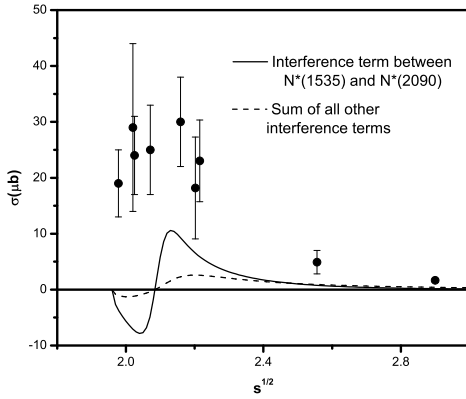
respectively, because the former is much larger than the later. The fitted curves are plotted by solid curves in Figs. 3 (a) and (b), respectively. They are obtained by summing over the contributions from all the  $N^*$  states coherently.



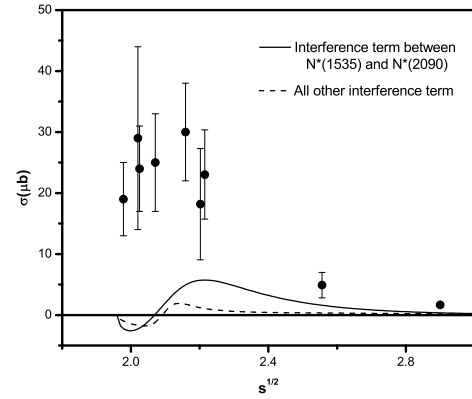
(a) Type I ( $\Gamma_{N^*(1900)}/\Gamma_{N^*(2090)}/\Gamma_{N^*(2100)} = 498\text{MeV}/95\text{MeV}/260\text{MeV}$ )



(b) Type II ( $\Gamma_{N^*(1900)}/\Gamma_{N^*(2090)}/\Gamma_{N^*(2100)} = 180\text{MeV}/350\text{MeV}/113\text{MeV}$ )



(c) Type I ( $\Gamma_{N^*(1900)}/\Gamma_{N^*(2090)}/\Gamma_{N^*(2100)} = 498\text{MeV}/95\text{MeV}/260\text{MeV}$ )



(d) Type II ( $\Gamma_{N^*(1900)}/\Gamma_{N^*(2090)}/\Gamma_{N^*(2100)} = 180\text{MeV}/350\text{MeV}/113\text{MeV}$ )

FIG. 3: Total cross section of the  $\pi^- p \rightarrow n\phi$  reaction.

From Fig. 3, we find that  $N_{1/2-}^*(1535)$  provides a major contribution in the whole energy range considered, especially near the  $N\phi$  threshold. The contribution from  $N_{3/2+}^*(1900)$  is relatively flat in the high energy region. The cross section from  $N_{1/2-}^*(2090)$  or  $N_{1/2+}^*(2100)$  has large uncertainty. Its shape depends on the total width of the state,  $\Gamma_{N^*}$ . If  $\Gamma_{N^*}$  is small, the cross section curve would show a relatively narrow peak around the mass of the

$N^*$ , otherwise it presents a broad structure. This is simply because that a Breit-Wigner form for the  $N^*$  propagator is adopted in the calculation. The  $P$  wave  $N_{1/2+}^*(2100)$  state can only play a minor role although it has a large branching fraction to  $N\eta$ , since its contribution near the  $N\phi$  threshold is too small. Furthermore, the contribution from  $N^*(2090)$  cannot be large because of a counter-contribution from the interference term between  $N^*(2090)$  and  $N^*(1535)$  in a region close to the  $N\phi$  threshold, namely a larger contribution from  $N^*(2090)$  makes the fit worse. In conclusion, although some higher resonances are introduced, the dominate contribution in the  $\pi^-p \rightarrow n\phi$  cross section still comes from the  $N_{1/2-}^*(1535)$  state, which is consistent with discussion in Ref. [8]. It should further be mentioned that the contribution from all the interference terms is about 2% only. Thus, the assumption that the contribution from ignored  $N^*$ s including their interference terms is about 10~15% of the total would be reasonable, and arranging the contributions from mentioned four  $N^*$ s in a range of 85~90% of the total will not affect our qualitative conclusion.

Based on the best fit, namely a small enough  $\chi^2$  and a reasonable overall fit, we can extract the coupling constant  $g_{N^*N\phi}^2$  for all adopted  $N^*$ s in all the mentioned cases. The resultant  $g_{N^*N\phi}^2$  for these  $N^*$ s are tabulated in Table II. The fractions of the individual contributions from all the considered  $N^*$ s are given in the table as well. From this table,

TABLE II: The extracted coupling constant  $g_{N^*N\phi}^2$  and the corresponding fraction of contribution in the  $\pi^-p \rightarrow n\phi$  reaction.

	$\Gamma_{N^*(1900)}/\Gamma_{N^*(2090)}/\Gamma_{N^*(2100)}$	$g_{\phi NN^*}^2(10^{-2})/(\text{fraction of contribution}(\%))$			
		$N_{1/2-}^*(1535)$	$N_{3/2+}^*(1900)$	$N_{1/2-}^*(2090)$	$N_{1/2+}^*(2100)$
type I	180MeV/95MeV/200MeV	140/67.1	7.92/0.9	0.937/3.6	12.3/13.5
	498MeV/95MeV/200MeV	137/64.9	1.14/1.0	1.19/4.8	9.46/9.8
	180MeV/95MeV/260MeV	128/61.7	3.53/0.4	1.37/5.6	10.8/15.4
	498MeV/95MeV/260MeV	126/60.0	0.758/0.8	1.27/4.7	11.7/16.4
type II	180MeV/350MeV/113MeV	116/55.2	6.41/0.7	0.749/4.4	16.2/23.3
	498MeV/350MeV/113MeV	115/52.6	0.656/0.7	0.967/5.4	17.0/23.1
	180MeV/414MeV/113MeV	118/56.2	3.27/0.4	1.13/3.7	17.5/24.8
	498MeV/414MeV/113MeV	114/54.0	0.783/0.7	1.05/3.3	18.6/25.7

one has following observations: (1)  $N_{1/2-}^*(1535)$  is a dominant resonance in the  $\pi^-p \rightarrow n\phi$

reaction and provides about 50% to 70% of the contribution. This state may couple to  $N\phi$  strongly, and the coupling constant  $g_{N^*(1535)N\phi}^2$  ranges from 1.1 to 1.4. The contribution and the coupling to  $N\phi$  in type I is larger than those in type II. (2) The  $N_{1/2+}^*(2100)$  state is the second largest contributor, which offers about 10% to 26% of the contribution. It also shows that  $N_{1/2+}^*(2100)$  may couple to  $N\phi$  remarkably. The value of the coupling constant  $g_{N^*(2100)N\phi}^2$  stretches from 0.09 to 0.19. And the contribution and the coupling to  $N\phi$  in type II is larger than those in type I. (3) The contribution from  $N_{1/2-}^*(2090)$  is about 3% to 6%, and  $g_{N^*(2090)N\phi}^2$  spans a range from 0.007 to 0.014. The contribution and the coupling to  $N\phi$  in type I is slightly larger than those in type II. (4) The contribution from  $N_{3/2+}^*(1900)$  is even smaller, about 0.4 % to 1.0%, and  $g_{N^*(1900)N\phi}^2$  spreads in a range of 0.006 to 0.079. The effect from the total width uncertainty of this state is quite small. These observations are clearly consistent with the information from the curves shown in Fig. 3. Namely,  $N_{1/2+}^*(2100)$  gives a contribution comparable to that from  $N_{1/2-}^*(1535)$ , especially in the higher energy region,  $N_{1/2-}^*(2090)$  offers a visible contribution around the energy about its mass, and  $N_{3/2+}^*(1900)$  only provides a very small contribution in the whole energy region.

Next, we determine  $g_{\psi NN^*}^2$  in terms of the partial decay widths of the  $J/\psi \rightarrow p\bar{p}\eta$  and  $J/\psi \rightarrow p\bar{n}\pi^-$  processes, respectively. The partial wave analysis of the  $J/\psi \rightarrow p\bar{p}\eta$  data collected at BESII shows that the partial decay width contributed by the intermediate  $N_{1/2-}^*(1535)$  state is about  $(56 \pm 15)\%$  [11]. By fitting this width, one can easily obtain the value of  $g_{\psi NN^*(1535)}^2$ . Again, a form factor with  $\Lambda$  being 1.8GeV in Eq.(15) is adopted in the calculation to describe the off-shell effect of  $N_{1/2-}^*(1535)$ , and the extracted  $g_{\psi NN^*(1535)}^2$  is tabulated in Table III. On the other hand, one notices that in analyzing the  $J/\psi \rightarrow p\bar{n}\pi^-$  data of BESII, assuming the contributions from  $N_{3/2+}^*(1900)$ ,  $N_{1/2-}^*(2090)$  and  $N_{1/2+}^*(2100)$  to be about 5~10%, respectively, are reasonable, and the resultant branching fraction of this channel is about  $(1.33 \pm 0.02(stat.)) \times 10^{-3}$  [12]. Therefore, we also approximately take the contributions from  $N_{1/2-}^*(1535)$ ,  $N_{3/2+}^*(1900)$ ,  $N_{1/2-}^*(2090)$  and  $N_{1/2+}^*(2100)$  to be 56%, 10%, 10% and 10%, respectively, in the calculation of the  $J/\psi \rightarrow p\bar{n}\pi^-$  decay. Using these assumptions, the extracted  $g_{\pi NN^*(1535)}^2$  values and the form factor in Eq.(15) with  $\Lambda$  being 1.8GeV for  $N_{1/2-}^*(1535)$  and 2.3GeV for either  $N_{3/2+}^*(1900)$ , or  $N_{1/2-}^*(2090)$  or  $N_{1/2+}^*(2100)$ , we can extract  $g_{\psi NN^*}^2$  for later three  $N^*$ s from the the branching fraction of the  $J/\psi \rightarrow p\bar{n}\pi^-$  decay. The resultant  $g_{\psi NN^*}^2$  and corresponding  $\Lambda$  are tabulated in Table III. From this table, we find that  $g_{\psi NN^*(1535)}^2$  is in the order of  $10^{-6}$ . Based on the ranges of the measured total

TABLE III:  $g_{\psi NN^*}^2$  and  $\Lambda$  for  $N_{1/2-}^*(1535)$ ,  $N_{3/2+}^*(1900)$ ,  $N_{1/2-}^*(2090)$  and  $N_{1/2+}^*(2100)$ .

$N^*$	Total Width(GeV)	$g_{\psi NN^*}^2$	
		$\Lambda=1.8\text{GeV}$	$\Lambda=2.3\text{GeV}$
$N_{1/2-}^*(1535)$	0.150	$1.319 \times 10^{-6}$	——
$N_{3/2+}^*(1900)$	0.180	——	$2.422 \times 10^{-5}$
	0.498	——	$7.744 \times 10^{-6}$
$N_{1/2-}^*(2090)$	0.095	——	$4.726 \times 10^{-5}$
	0.350	——	$1.612 \times 10^{-5}$
	0.414	——	$2.830 \times 10^{-5}$
$N_{1/2+}^*(2100)$	0.113	——	$1.362 \times 10^{-5}$
	0.200	——	$2.290 \times 10^{-5}$
	0.260	——	$2.031 \times 10^{-5}$

width and the obtained  $g_{\pi NN^*}^2$  for the  $N_{3/2+}^*(1900)$ ,  $N_{1/2-}^*(2090)$ , and  $N_{1/2+}^*(2100)$  states, the extracted values of  $g_{\psi NN^*(1900)}^2$ ,  $g_{\psi NN^*(2090)}^2$ , and  $g_{\psi NN^*(2100)}^2$  could vary in the ranges of  $(0.77 \sim 2.4) \times 10^{-5}$ ,  $(1.6 \sim 4.7) \times 10^{-5}$ , and  $(1.4 \sim 2.3) \times 10^{-5}$ , respectively. It seems that the couplings of  $J/\psi$  to  $N$  and different  $N^*$  are about the same. This is understandable, because that  $J/\psi$  is merely composed of charmed quarks,  $N$  is consist of upper and down quarks only, and  $N^*$  is made up of upper, down and even strange quarks, thus the coupling mechanisms for different  $N^*$ s would be the same.

In terms of the extracted the values of  $g_{\psi NN^*}^2$  and  $g_{\phi NN^*}^2$ , we are in the stage of calculating physics observables in the  $J/\psi \rightarrow p\bar{p}\phi$  decay with adopted intermediate states  $N_{1/2-}^*(1535)$ ,  $N_{3/2+}^*(1900)$ ,  $N_{1/2-}^*(2090)$  and  $N_{1/2+}^*(2100)$ . The resultant invariant mass spectra of  $p\phi$  are plotted in Fig. 4. In sub-figures (a) and (b), the dashed and solid curves represent the upper and lower limits of the total invariant mass spectrum, which are caused by the uncertainties of the widths of the  $N_{3/2+}^*(1900)$ ,  $N_{1/2-}^*(2090)$  and  $N_{1/2+}^*(2100)$  states. And in sub-figures (c) and (d), the dashed, dotted, dash-dotted and dash-double-dotted curves describe the sub-contributions from the  $N_{1/2-}^*(1535)$ ,  $N_{3/2+}^*(1900)$ ,  $N_{1/2-}^*(2090)$  and  $N_{1/2+}^*(2100)$  states, respectively. The fractions of the contributions for these  $N^*$ s in the decay are tabulated in Table IV.

From the numerical values in Table IV and the  $p\phi$  invariant mass curves in Fig. 4, we have



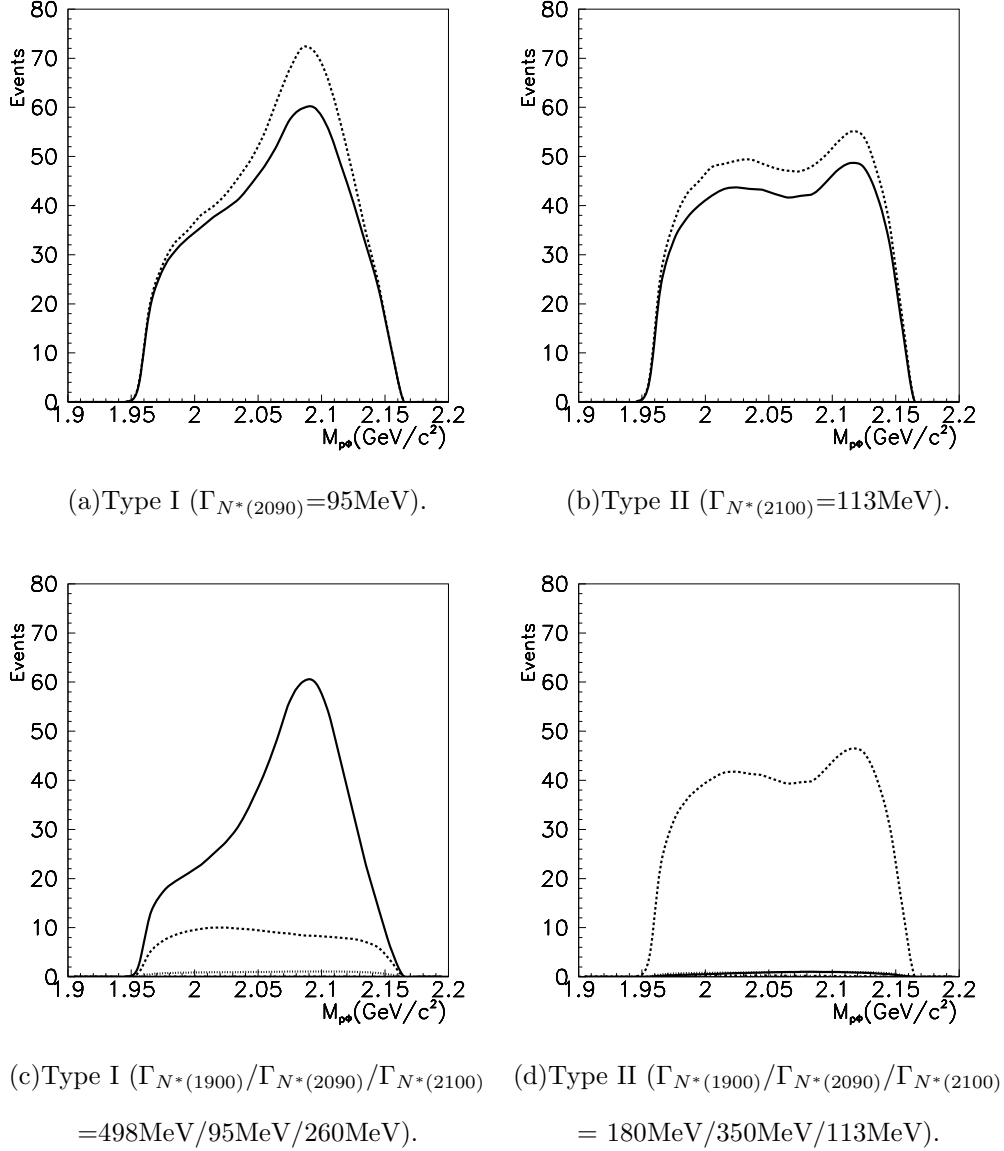


FIG. 4: Invariant mass spectra of  $p\phi$  in type I ( $\Gamma_{N^*(2100)}=113\text{MeV}$ ) and type II ( $\Gamma_{N^*(2090)}=95\text{MeV}$ ) with two curves covering the range of 4 sets of parameters. In (c) and (d), the solid-line is from  $N^*(2090)$ 's contribution; the dash-line is from  $N^*(2100)$ 's; the dash-dotted line is from  $N^*(1535)$ 's; the dash-dotted-dotted line is from  $N^*(1900)$ 's.

following observations. From Fig. 4(a) and Table IV, one sees that in type I the contribution from  $N_{1/2}^*(2090)$  is about  $(46.3\sim 72.1)\%$ , and there is a peak structure around  $2.09\text{GeV}$ . The sub-contributions from various  $N^*$ 's shown in Fig. 4(c) tell us that this structure is mainly contributed by  $N_{1/2}^*(2090)$  due to its relatively narrow width, namely a stronger coupling between  $N$  and  $\phi$ . This implies that there may exists a large  $N\phi$  or  $qqqs\bar{s}$  compo-

TABLE IV: Fractions of contributions from  $N_{1/2-}^*(1535)$ ,  $N_{3/2+}^*(1900)$ ,  $N_{1/2-}^*(2090)$  and  $N_{1/2+}^*(2100)$  in the  $J/\psi \rightarrow p\bar{p}\phi$  decay.

	$\Gamma_{N^*(1900)} / \Gamma_{N^*(2090)} / \Gamma_{N^*(2100)}$	fraction(%)			
		$N^*(1535)$	$N^*(1900)$	$N^*(2090)$	$N^*(2100)$
type I	180MeV/95MeV/200MeV	2.01	0.44	48.22	32.80
	498MeV/95MeV/200MeV	1.96	0.01	61.24	25.23
	180MeV/95MeV/260MeV	1.83	0.20	70.51	15.12
	498MeV/95MeV/260MeV	1.81	0.01	65.36	16.38
type II	180MeV/350MeV/113MeV	1.66	0.36	1.42	76.26
	498MeV/350MeV/113MeV	1.65	0.01	1.83	80.03
	180MeV/414MeV/113MeV	1.69	0.18	2.72	82.38
	498MeV/414MeV/113MeV	1.63	0.01	2.53	87.56

nent in  $N_{1/2-}^*(2090)$ . Meanwhile the  $N_{1/2+}^*(2100)$  state also provides a sizable contribution of about (15.1~32.8)%, but this contribution is smaller than that offered by  $N_{1/2-}^*(2090)$ , and the shape of the contribution is flatter due to a large width of the state. Therefore, this piece of contribution would not affect the shape of the total contribution qualitatively. The contributions from  $N_{1/2-}^*(1535)$  and  $N_{3/2+}^*(1900)$  are negligibly small, their contributions are about (1.81~2.00)% and (0.01~0.44)%, respectively. The interference terms can only provide about 2% of the contribution. Therefore, disregarding the contributions from the  $N_{1/2-}^*(1535)$  and  $N_{3/2+}^*(1900)$  states and the interference terms will not affect the conclusion qualitatively. From Fig. 4(b) and Table IV, one finds that in type II the contribution from  $N_{1/2+}^*(2100)$  is about (76.3~87.6)%, and there is also a small peak structure around 2.11GeV. The sub-contributions plotted in Fig. 4(d) show that this structure almost entirely comes from contribution of  $N_{1/2+}^*(2100)$ , because of its dominant contribution and relatively narrow width. This also implies that its coupling to  $N\phi$  could be remarkable, a significant  $N\phi$  or  $qqqs\bar{s}$  component may exist in  $N_{1/2+}^*(2100)$ . Meanwhile the contributions from  $N_{1/2-}^*(1535)$ ,  $N_{3/2+}^*(1900)$  and  $N_{1/2-}^*(2090)$  are negligibly small, their contributions are about (1.63~1.70)%, (0.01~0.36)% and (1.33~2.65)%, respectively. The interference terms can only give a contribution about 2%. It also shows that one would not be able to explore the possible strange structures for  $N_{1/2-}^*(1535)$  and  $N_{3/2+}^*(1900)$  in the type I case and for

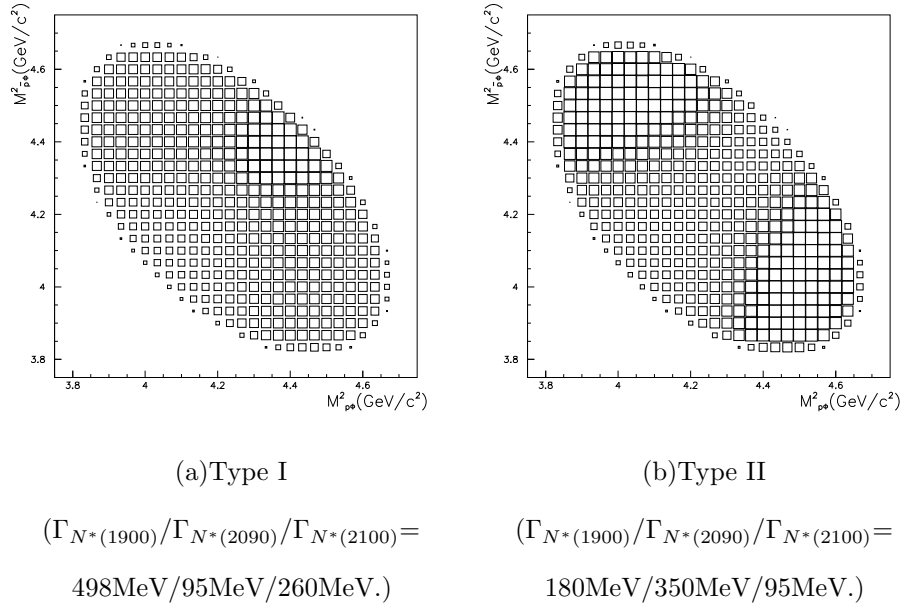


FIG. 5: Dalitz plots.

$N_{1/2-}^*(1535)$ ,  $N_{3/2+}^*(1900)$  and  $N_{1/2-}^*(2090)$  in the type II case in this decay process, because their informations are deeply submerged in the signals of the  $N_{1/2-}^*(2090)$  and  $N_{1/2+}^*(2100)$  states and the  $N_{1/2+}^*(2100)$  state, respectively.

Furthermore, the Dalitz plots for type I and type II are plotted in Fig.5. It is shown that the Dalitz plots of types I and II have distinguishable features. In the type I case, there are one vertical belt and one horizontal belt at  $4.37(\text{GeV}/c^2)^2$  and an enhancement in the upper right corner. But in the type II case, there is only two enhancements at the upper left and lower right corners. These patterns agree with the findings from the invariant mass curves.

Finally, we need to mention that the value of the cut-off parameter in a certain range does not qualitatively affect our conclusion.

#### IV. SUMMARY

In this paper, the  $J/\psi \rightarrow p\bar{p}\phi$  decay is studied in the isobar resonance model with effective Lagrangians. In such a model, the nucleon resonances are adopted as the intermediate states. Because of the  $s\bar{s}$  structure of the  $\phi$ -meson and the OZI rule, the major decay width of this process will be contributed by the resonances who contain strange content. Therefore, this decay process could be used to study the possible strange structure of the nucleon resonances.

Based on a careful analysis, four  $N^*$  states,  $N_{1/2-}^*(1535)$ ,  $N_{3/2+}^*(1900)$ ,  $N_{1/2-}^*(2090)$  and  $N_{1/2+}^*(2100)$ , are adopted in the calculation, so that the qualitative conclusion would not be affected. The coupling constants  $g_{\pi NN^*}^2$  for these  $N^*$ s and  $g_{\eta NN^*}^2$  for  $N_{1/2-}^*(1535)$  are extracted from the branching fractions of the  $N^*$ s to the  $N\pi$  channel and of  $N_{1/2-}^*(1535)$  to the  $N\eta$  channel, respectively, in the first step. With determined  $g_{\pi NN^*}^2$ , coupling constant  $g_{\phi NN^*}^2$  for  $N^*$ s are obtained by fitting the cross section of the  $\pi^- p \rightarrow n\phi$  reaction. Because the uncertainties of the partial width for  $N_{3/2+}^*(1900)$ ,  $N_{1/2-}^*(2090)$  and  $N_{1/2+}^*(2100)$ , the resultant  $g_{\phi NN^*}^2$ s are allowed to change in certain regions. It is found that in the best fit, except the dominant contribution from  $N_{1/2-}^*(1535)$  and negligible contribution from  $N_{3/2+}^*(1900)$ , the contributions from  $N_{1/2-}^*(2090)$  and  $N_{1/2+}^*(2100)$  are visible and even remarkable in some cases, and the total widths of these two states cannot be large simultaneously. Therefore, there are two types of fits. In the first type, type I,  $N_{1/2-}^*(2090)$  and  $N_{1/2+}^*(2100)$  have a smaller total width and a larger total width, respectively, and in the second type, type II, it is the other way round. In the second step, the coupling constant  $g_{\psi NN^*(1535)}^2$  and  $g_{\psi NN^*}^2$  for other three  $N^*$ s are extracted by fitting the partial decay widths of the  $J/\psi \rightarrow p\bar{p}\eta$  process and the  $J/\psi \rightarrow p\bar{n}\pi^-$  process, respectively.

Finally, we can calculate the physical observables in the  $J/\psi \rightarrow p\bar{p}\phi$  decay by using obtained  $g_{\pi NN^*}^2$ s and  $g_{\psi NN^*}^2$ s in the type I and type II cases. The invariant mass spectrum of  $p\phi$  in the type I case shows that there is a peak structure around 2.09GeV due to the major contribution from the narrower  $N_{1/2-}^*(2090)$  state. This means that its coupling to  $N\phi$  is relatively strong, and a large  $N\phi$  or  $qqqs\bar{s}$  component may exist in  $N_{1/2-}^*(2090)$ . Meanwhile the contribution from  $N_{1/2+}^*(2100)$  is flatter and smaller, which implies that even there is a strange ingredient in this state, its coupling to  $N\phi$  would be weaker. In the type II case, the curve of the invariant mass spectrum of  $p\phi$  has a small peak structure around 2.11GeV, because of the dominant contribution from the narrow  $N_{1/2+}^*(2100)$  state and negligible contributions from other states. It suggests that its coupling to  $N\phi$  is strong, a significant  $N\phi$  or  $qqqs\bar{s}$  component might exist in the  $N_{1/2+}^*(2100)$ . However, one would not be able to reveal the strange structure in  $N_{1/2-}^*(2090)$ , because its information is deeply submerged in the signal of the  $N_{1/2+}^*(2100)$  state. For the same reason, no matter in which cases, one cannot figure out strange structures of  $N_{1/2-}^*(1535)$  and  $N_{3/2+}^*(1900)$  from this process.

In summary, in the  $J/\psi \rightarrow p\bar{p}\phi$  decay, the widths of  $N_{1/2-}^*(2090)$  and  $N_{1/2+}^*(2100)$

cannot be large simultaneously. The proposed study of this channel with the high statistics BESIII data [21] will tell us how the  $p\phi$  invariant mass curve goes. If the shape of the curve likes that of type I, the width of the  $N_{1/2-}^*(2090)$  state is narrower and there would be a considerable amount of  $p\phi$  or  $qqqs\bar{s}$  component in the state, while the width of the  $N_{1/2+}^*(2100)$  state would be wider. If the shape of the curve is similar to that of type II, only the width of the  $N_{1/2+}^*(2100)$  state is narrower and there would be a certain amount of  $p\phi$  or  $qqqs\bar{s}$  component in the state. Of course, the real data of high statistics on the  $J/\psi \rightarrow p\bar{p}\phi$  decay may reveal more knowledge on all possible  $N^*$ s than our predictions based on the information from  $\pi N \rightarrow \phi N$ . It will definitely provide us useful information on the  $N^*$  resonances with large  $qqqs\bar{s}$  component. And the  $pp \rightarrow pp\phi$  reaction should also be studied to confirm our prediction.

### Acknowledgments

This work is partly supported by the National Natural Science Foundation of China under grants Nos. 10875133, 10847159, 10975038, 11035006, 11165005, and the Key-project by the Chinese Academy of Sciences under project No. KJCX2-EW-N01, and the Ministry of Science and Technology of China (2009CB825200).

- 
- [1] B.C. Liu, B.S. Zou, Phys. Rev. Lett. **96**, 042002 (2006);  
B.C. Liu, B.S. Zou, Phys. Rev. Lett. **98**, 039102 (2007).
  - [2] B.C. Liu, B.S. Zou, Commun. Theor. Phys. **46**, 501 (2006).
  - [3] G. Penner and U. Mosel, Phys. Rev. **C66**, 055211 (2002); *ibid.* **C66**, 055212 (2002);  
V. Shklyar, H. Lenske and U. Mosel, Phys. Rev. **C72**, 015210 (2005).
  - [4] B. Julia-Diaz, B. Saghai, T. S. H. Lee and F. Tabakin, Phys. Rev. **C73**, 055204 (2006).
  - [5] M. Q. Tran et al., Phys. Lett. **B445**, 20 (1998);  
K. H. Glander et al., Eur. Phys. J. **A19**, 251 (2004).
  - [6] J. W. C. McNabb et al., Phys. Rev. **C62**, 042201(R) (2004).
  - [7] S. Okubo, Phys. Lett. **5**, 165 (1963);  
G. Zweig, CERN report Th-412 (1964);  
J. Iizuka, Prog. Theor. Phys. Suppl. **38**, 21 (1966).

- [8] J. J. Xie, B. S. Zou and H.C. Chiang, Phys. Rev. **C77**, 015206 (2008) (and reference therein).
- [9] J. E. Augusttin et al., (DM2 Collaboration), Phys. Rev. Lett. **60**, 2238 (1988).
- [10] A. Baldini et al., *Total Cross Sections of High Energy Particles: Landolt – Börnstein, Numerical Data and Functional Relationships in Science an Technology*, edited by H. Schopper, (Springer-Verlag, New York, 1988), *vol. 12*.
- [11] J. Z. Bai et al., (BES Collaboration), Phys. Lett. **B510**, 75 (2001).
- [12] M. Ablikim et al., (BES Collaboration), Phys. Rev. Lett. **97**, 062001 (2006).
- [13] A. Sibirtsev, J. Haidenbauer, U.-G. Meissner, Eur. Phys. J. A **27**, 263 (2006); A. Sibirtsev, W. Cassing, *ibid* **7**, 407 (2000); A.I. Titov, B. Kämpfer, and B. L. Reznik, Eur. Phys. J. A **7**, 543 (2000); K. Tsushima, K.Nakayama, Phys. Rev. **C68**, 034612 (2003); L.P. Kaptari, B. Kämpfer, Eur. Phys. J. A **23**, 291 (2005).
- [14] K. Tsushima, A. Sibirtsev, A. W. Thomas Phys. Lett. **B390**, 29 (1997) (and reference therein).
- [15] A. I. Titov, B. Kämpfer, and B. L. Reznik, Phys. Rev. **C65**, 065022 (2002) (and reference therein).
- [16] G. Penner and U. Mosel, Phys. Rev. **C66**, 055211 (2002); *ibid.* **C66**, 055212 (2002); V. Shklyar, H. Lenske and U. Mosel, Phys. Rev. **C72**, 015210 (2005).
- [17] T. Feuster and U. Mosel, Phys. Rev. **C58**, 457 (1998); **C59**, 460 (1999).
- [18] W. H. Liang et al., J. Phys. **G28**, 333 (2002).
- [19] The Review of Particle Physics, C. Amsler et al., Phys. Lett. **B667**, 1 (2008).
- [20] M. Ablikim et al., (BES Collaboration), Phys. Rev. **D80**, 052004 (2009).
- [21] D. M. Asner, T. Barnes, J. M. Bian, I. I. Bigi, N. Brambilla, I. R. Boyko, V. Bytev, K. T. Chao *et al.*, “Physics at BES-III”, [arXiv:0809.1869 [hep-ex]]; private talk with Prof.H.C.Chiang and Prof.W.H.Liang, 2007

## APPENDIX

### Appendix A

The invariant amplitudes of  $\pi^- p \rightarrow n\phi$  reaction with  $N^*(1535)$ ,  $N^*(1900)$ ,  $N^*(2090)$  and  $N^*(2100)$  being intermediate states are as follows:

For  $N^*(1535)$

$$\mathcal{M}_{N^*(1535)} = \sqrt{2}g_{\pi NN^*}g_{\phi NN^*}F_{N^*}(q^2)\bar{u}(p_n, s_n)\gamma_5(\gamma_\nu - \frac{q_\nu \not{q}}{q^2})\epsilon^\nu(p_\phi, s_\phi)G_{N^*}(q)u(p_p, s_p), \quad (\text{A1})$$

for  $N^*(1900)$

$$\mathcal{M}_{N^*(1900)} = \frac{i\sqrt{2}}{M_{N^*}}g_{\pi NN^*}g_{\phi NN^*}F_{N^*}(q^2)\bar{u}(p_n, s_n)\gamma_5\epsilon_\mu(p_\phi, s_\phi)G_{N^*}^{\mu\nu}(q)p_{\pi\nu}u(p_p, s_p), \quad (\text{A2})$$

For  $N^*(2090)$

$$\mathcal{M}_{N^*(2090)} = \sqrt{2}g_{\pi NN^*}g_{\phi NN^*}F_{N^*}(q^2)\bar{u}(p_n, s_n)\gamma_5(\gamma_\nu - \frac{q_\nu \not{q}}{q^2})\epsilon^\nu(p_\phi, s_\phi)G_{N^*}(q)u(p_p, s_p), \quad (\text{A3})$$

and for  $N^*(2100)$

$$\mathcal{M}_{N^*(2100)} = i\sqrt{2}g_{\pi NN^*}g_{\phi NN^*}F_{N^*}(q^2)\bar{u}(p_n, s_n)\gamma_\nu\epsilon^\nu(p_\phi, s_\phi)G_{N^*}(q)\gamma_5u(p_p, s_p), \quad (\text{A4})$$

where  $p_\pi$  is the four momentum of  $\pi^-$  meson, and  $\epsilon(p_\phi)$  is the polarization vector of  $\phi$  meson.

### Appendix B

The invariant amplitude of  $J/\psi \rightarrow p\bar{p}\eta$  decay with  $N^*(1535)$  being the intermediate state is written as:

$$\begin{aligned} \mathcal{M}_{N^*(1535)} = & ig_{\eta NN^*}g_{\psi NN^*}\bar{u}(p_1, s_1)[G_{N^*}(q)F_N(q^2)\gamma_5\sigma_{\mu\rho}p_\psi^\rho\epsilon^\mu(k, s_\psi) \\ & + \gamma_5\sigma_{\mu\rho}p_\psi^\rho\epsilon^\mu(k, s_\psi)G_{\bar{N}^*}(q')F_N(q'^2)]v(p_2, s_2), \end{aligned} \quad (\text{B1})$$

with  $p_\psi$  and  $\epsilon(p_\psi)$  being the four momentum and the polarization vector of  $J/\psi$ .

The invariant amplitudes of  $J/\psi \rightarrow p\bar{n}\pi^-$  reaction with  $N^*(1900)$ ,  $N^*(2090)$  and  $N^*(2100)$  being intermediate states are as follows:

For  $N^*(1900)$ ,

$$\mathcal{M}_{N^*(1900)} = \frac{i\sqrt{2}}{M_{N^*}}g_{\pi NN^*}g_{\psi NN^*}\bar{u}(p_1, s_1)\gamma_5\epsilon_\mu(k, s_\psi)G_{N^*}^{\mu\nu}(q')F_N(q'^2)p_{\pi\nu}v(p_2, s_2). \quad (\text{B2})$$

For  $N^*(2090)$ ,

$$\mathcal{M}_{N^*(2090)} = i\sqrt{2}g_{\pi NN^*}g_{\psi NN^*}\bar{u}(p_1, s_1)\gamma_5\sigma_{\mu\rho}p_\psi^\rho\epsilon^\mu(k, s_\psi)G_{\bar{N}^*}(q')F_N(q'^2)v(p_2, s_2). \quad (\text{B3})$$

For  $N^*(2100)$ ,

$$\mathcal{M}_{N^*(2100)} = i\sqrt{2}g_{\pi NN^*}g_{\psi NN^*}\bar{u}(p_1, s_1)\gamma_\mu\epsilon^\mu(k, s_\psi)G_{\bar{N}^*}(q')F_N(q'^2)\gamma_5v(p_2, s_2). \quad (\text{B4})$$

### Appendix C

The invariant amplitudes of  $J/\psi \rightarrow p\bar{p}\phi$  decay with  $N^*(1535)$ ,  $N^*(1900)$ ,  $N^*(2090)$  and  $N^*(2100)$  being intermediate states are as follows:

For  $N^*(1535)$ ,

$$\begin{aligned} \mathcal{M}_{N^*(1535)} = & ig_{\phi NN^*}g_{\psi NN^*}\bar{u}(p_1, s_1)[\gamma_5(\gamma_\nu - \frac{q_\nu \not{q}}{q^2})\epsilon^\nu(p_3, s_\phi)G_{N^*}(q)F_N(q^2)\gamma_5\sigma_{\mu\rho}p_\psi^\rho\epsilon^\mu(k, s_\psi) \\ & + \gamma_5\sigma_{\mu\rho}p_\psi^\rho\epsilon^\mu(k, s_\psi)G_{\bar{N}^*}(q')F_N(q'^2)\gamma_5(\gamma_\nu - \frac{q'_\nu \not{q}'}{q'^2})\epsilon^\nu(p_3, s_\phi)]v(p_2, s_2). \end{aligned} \quad (\text{C1})$$

For  $N^*(1900)$ ,

$$\begin{aligned} \mathcal{M}_{N^*(1900)} = & -g_{\phi NN^*}g_{\psi NN^*}\bar{u}(p_1, s_1)[\gamma_5\epsilon_\nu(p_3, s_\phi)G_{N^*}^{\nu\mu}(q)F_N(q^2)\gamma_5\epsilon_\mu(k, s_\psi) \\ & + \gamma_5\epsilon_\mu(k, s_\psi)G_{\bar{N}^*}^{\mu\nu}(q')F_N(q'^2)\gamma_5\epsilon_\nu(p_3, s_\phi)]v(p_2, s_2). \end{aligned} \quad (\text{C2})$$

For  $N^*(2090)$ ,

$$\begin{aligned} \mathcal{M}_{N^*(2090)} = & ig_{\phi NN^*}g_{\psi NN^*}\bar{u}(p_1, s_1)[\gamma_5(\gamma_\nu - \frac{q_\nu \not{q}}{q^2})\epsilon^\nu(p_3, s_\phi)G_{N^*}(q)F_N(q^2)\gamma_5\sigma_{\mu\rho}p_\psi^\rho\epsilon^\mu(k, s_\psi) \\ & + \gamma_5\sigma_{\mu\rho}p_\psi^\rho\epsilon^\mu(k, s_\psi)G_{\bar{N}^*}(q')F_N(q'^2)\gamma_5(\gamma_\nu - \frac{q'_\nu \not{q}'}{q'^2})\epsilon^\nu(p_3, s_\phi)]v(p_2, s_2). \end{aligned} \quad (\text{C3})$$

For  $N^*(2100)$ ,

$$\begin{aligned} \mathcal{M}_{N^*(2100)} = & g_{\phi NN^*}g_{\psi NN^*}\bar{u}(p_1, s_1)[\gamma_\nu\epsilon^\nu(p_3, s_\phi)G_{N^*}(q)F_N(q^2)\gamma_\mu\epsilon^\mu(k, s_\psi) \\ & + \gamma_\mu\epsilon^\mu(k, s_\psi)G_{\bar{N}^*}(q')F_N(q'^2)\gamma_\nu\epsilon^\nu(p_3, s_\phi)]v(p_2, s_2). \end{aligned} \quad (\text{C4})$$